3-D Printed dual-band Microwave Imaging Antenna

Vamsi Borra[a,*], Srikanth Itapu[b], Joao Garretto[a], Ronald J. Yarwood[a], Gina E. Morrison[c], Pedro Cortes[c], Eric MacDonald[d] and Frank Li[a]

[a] Electrical and Computer Engineering, Youngstown State University, Ohio 44555, USA.
[b] Department of ECE, Alliance University, Bengaluru, Karnataka 562106, India
[c] Chemical Engineering, Youngstown State University, Ohio 44555, USA
[d] Mechanical Engineering, University of Texas at El Paso, El Paso, Texas 79968, USA

*Correspondence: vsborra@ysu.edu

Microwave imaging utilizes low-power Near-field electromagnetic fields at microwave frequencies to detect the internal structure of an object. Sufficient resolution through the thickness is crucial in biomedical applications to detect small objects of concern. Parameters such as the frequency of microwave signals, the design, and the material of the antenna are the most important factors to consider for microwave-based biomedical sensing. The proposed antenna falls under the good health and well-being goal, which is among the sustainable development goals (SDGs) that transform the world and yields merits of: compactness in size, ease of fabrication, wider impedance bandwidth, simple design, and good RF performance. An Asymmetric-fed Coupled Stripline (ACS) antenna is 3D-printed on an FR4 substrate with return loss measurements ranging from 2 GHz to 20 GHz. The impedance bandwidth is obtained between 6 GHz to 8 GHz and 15 GHz to 17 GHz. The proposed microwave antenna was simulated using Ansys HFSS. The parameters are designed to ensure optimum radiation efficiency. The radiation patterns obtained were omnidirectional in H-plane and bidirectional in E-plane.

Introduction

Implantable antennas are an area of significant scientific interest, due to their importance within medical implant technologies, such as wireless sensors, stimulators, and others. Its design is associated with several limiting factors, that include miniaturization, insertion loss through the human body, regulation guidelines, and biocompatibility. Initial research on implantable antennas focused on the design of linear polarized antennas. Due to the invisibility of the implant inside the human body, it is difficult to precisely detect the orientation of the implantable antenna. Therefore, according to[1], circular polarization (CP) is preferred for implantable antennas to establish effective and efficient communication. The authors propose a low-profile ring antenna with a compact size at 2.4 and 2.48 GHz ISM bands for biomedical applications. It is initially developed as a simple patch antenna, with the performance of the CP being modeled through the

introduction of shorting pins and an L-shaped open-end slot. After a patch-loaded Pin-Loaded Angular Ring Antenna (PLAR) structure is adopted as a modification to generate two closely spaced resonances.

As previously mentioned, wireless communication is an active research topic in health care and biomedical applications, which can translate and complement the sustainable development goals (SDGs) transforming the world. Wireless Capsule Endoscopy (WCE) is an ingestible medical device that captures images while traveling through the human gastrointestinal tract and has become a popular alternative to regular endoscopy. As the antenna plays a vital role in WCE systems, limitations such as the dimensions of the antenna, and its low-speed data communication are currently researched to make such devices more efficient. In [2], an Ultrawide-Band PIFA antenna is designed and optimized for compact size. Defected ground layer and H-shaped patch are introduced for bandwidth enhancement. Simulation results showed that the antenna resonates at the frequency of 6.22 GHz, with the magnitude of the reflection coefficient to be -33 dB, indicating good matching of the antenna.

The understanding of signal propagation within the human body tissues is an important factor in the design of wireless medical monitoring systems. The propagation loss in the human body tissues increases significantly at higher frequencies, on the other hand, the design of very small and efficient antennas for implants is of increased difficulty at lower frequencies, presenting a lower resolution for complex applications such as detecting small tumors or brain hemorrhages. In[3], the research extends the study of wireless signal coverage from a directional bio-matched on-body antenna inside the abdominal and intestine area at several frequencies. The study and simulation were performed by placing a mini-horn antenna on the center area of the abdomen and a capsule antenna is placed inside the small intestine at two different locations. The research concludes that directional on-body antennas could enable the utilization of higher frequency bands for implant communications if carefully placed. In addition, although the directionality of these antennas implies deeper tissue penetration, the possibility of smaller 3D coverage might necessitate more numbers of antennas to cover a certain region inside the human body.

In [4], a miniaturized circular-shaped patch antenna is proposed, using FR4 as the dielectric material, with highly compact sized constrained for biomedical applications. The partial ground structure was used to obtain the required wide bandwidth and the height of the ground was designed to be 3mm in order to achieve a reflection coefficient value of -37 dB at a frequency of 5 GHz. Simulations results presented a resonance frequency of 5.7 GHz with a bandwidth performance of 11.2 GHz. In [5], the authors fabricated an ACS fed monopole antenna for 2 - 2.5 GHz, 3.5 - 3.7 GHz. and 5.5 - 6.75 GHz. These three are selected as they can effectively cover usages in WLAN (2.4/5.8) and WiMAX (3.5). These are desirable bands in mobile applications so to have one compact design is better than having multiple. ACS was decided as the foundation as they have been shown in other works to help in the reduction of size in wide-band applications. Similarly, the authors of [6] proposed a compact design with a rectangular-shaped split-ring resonator (RSRR). The proposed antenna operated in the WiBro (2.3 GHz), WLAN (2.4/5.2 GHz), WiMAX (2.5/5.5 GHz) X-band downlink (7.4 GHz) and

ITU bands (8.5 GHz). The RSRR was embedded along with the radiating element to obtain the middle band and to enhance impedance matching at the higher frequency band (metamaterial property). An electrically compact, ACS-fed reconfigurable antenna is developed for mobile handheld devices, which can operate at 5G mid-frequency band and LTE band-40 was proposed in [7]. Using a perfect switch and pin diode as a switch, the reconfigurability function was incorporated in the antenna design. Based on the switch ON and OFF state, the length of the radiating strip is altered. In terms of size, the proposed antenna geometry was $(16.5 \times 10.5 \times 1.6)$ mm^3. Ultra-wideband Antennas are also explored in [8]–[11] operating in the 3 - 10.6 GHz but were not applicable to 5G frequencies.

In this paper, we explore the capabilities of Asymmetrically Coupled Stripline (ACS)-fed microstrip antenna operating in the 2 - 20 GHz frequency range with compact size, i.e., 30 mm x 20 mm x 1.6 mm. The proposed antenna facilitates a dual-band operation best suited for biomedical imaging applications. The advantage of having a single-sided radiating element greatly reduces the fabrication cost.

Antenna Geometry and Fabrication

The proposed antenna shown in Fig. 2 consists of two radiating striplines, one with dimensions 23 mm x 2 mm and its asymmetric stripline with dimensions 12 mm x 2 mm separated by a distance of 0.5 mm. The antenna was fabricated on a virgin FR4 substrate (ε_r = 4.4) and a loss tangent of 0.02. An SMA connector with an impedance of 50Ω is soldered to the ACS-fed antenna for measurements. Simulations were performed using the Ansys HFSS Electronics Desktop v.20 (Fig. 2(a)). The antenna was fabricated using the Voltera V-One PCB printer, Fig. 1, with Silver conductive ink (from Voltera) (Fig. 2(b)). To start the process, a Gerber file was generated from the Ansys HFSS design. The file was later imported to the Voltera software. After uploading the file, proper steps were followed to complete the antenna print. The first step was to mount a measuring probe onto the printer to calibrate the size constraints of the 30 mm x 20 mm PCB board. After calibration, the silver ink conductor cartridge was positioned into a dispensing fixture. The conductor ink, manufactured by Voltera, was printed onto the board, and then cured at 240℃ for 1 hour. The board was given approximately 15 minutes to cool down. Two samples are presented here with their printing parameters optimized. The S_{11} characteristics of the two samples are measured to check the accuracy between simulated and measured results.

The measurements are validated using the Keysight E5080B ENA Vector Network Analyzer (VNA) which facilitates measurements from 20 MHz to 40 GHz. The SLOT (Short-Load-Open-Through) calibration in performed for faithful measurements on the VNA (Fig. 3).

Figure 1: Voltera V-One Desktop PCB Printer used for the fabrication of the antenna.

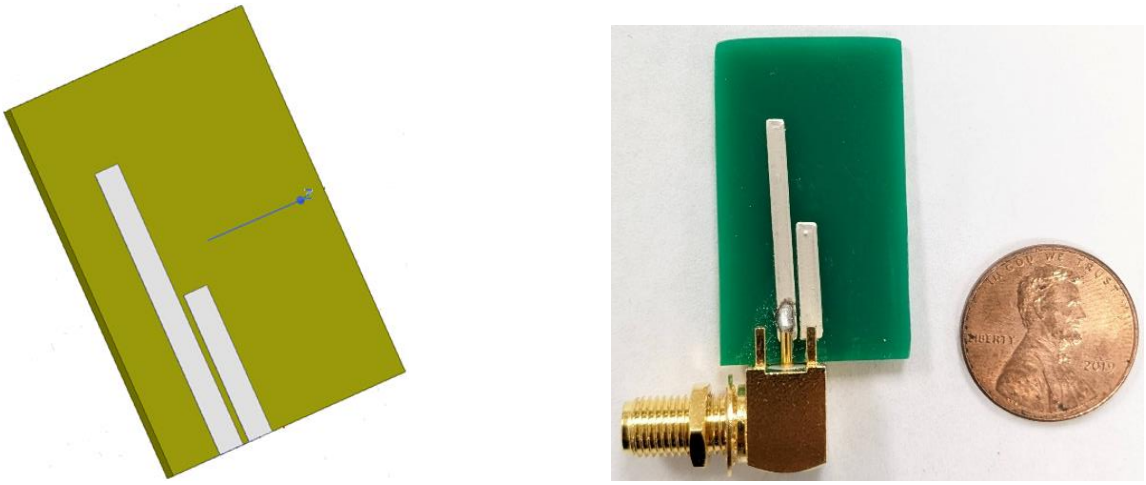

(a) (b)

Figure 2. The proposed ACS-fed Antenna. (a) Simulated in Ansys HFSS and (b) Printed Antenna using Voltera V-One Desktop PCB Printer.

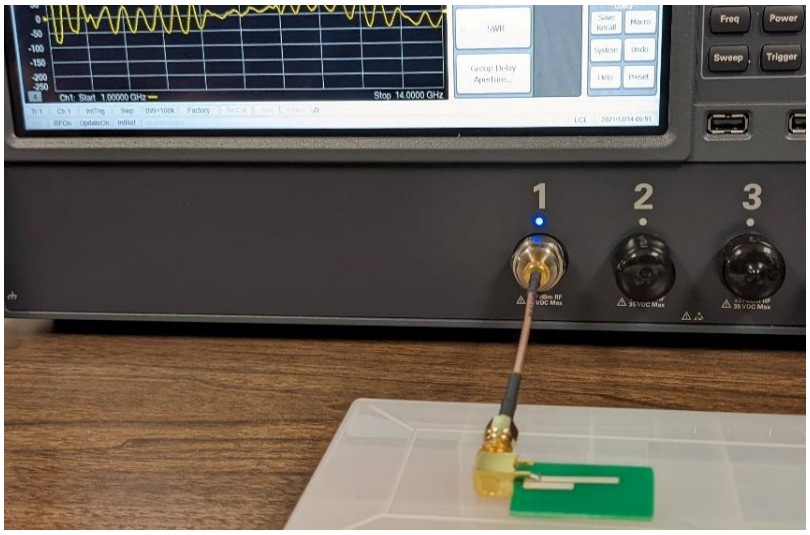

Figure 3. Antenna measurment setup on Keysight E5080B ENA VNA.

Results and Discussion

Fig. 4 and Fig. 5 depict both the simulated and measured S_{11} characteristics in (dB) over a wide frequency ranging from 2 GHz to 20 GHz. The Asymmetric Coupled feeds provide the necessary LC circuit equivalent at the lower frequency band (6 to 8 GHz) resulting in a highly resonant S_{11} of -25 dB. The distance between the feeds is optimized to 0.5 mm, thus avoiding any current crowding at the edges of the striplines. The printing parameters for the printer are optimized for the two antennas. The corresponding return loss is compared with the simulated results in figures 4 and 5. Here, the 6-8 GHz frequency is selected for personal healthcare (patient monitoring) in the IoT domain [12].

From Fig. 4, it can be deduced that the resonant frequency (at around 6.2 GHz) is slightly broadened when printed, as compared to the simulated return loss, thus suggesting that the requires some fine-tuning for printing and other parameters.

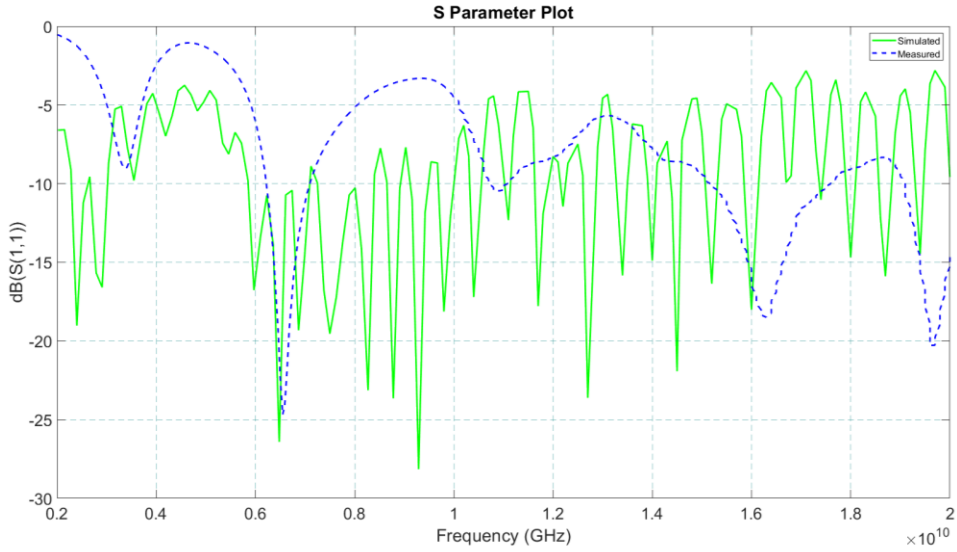

Figure 5. The simulated and measured return loss of the printed antenna-1.

From Fig. 5, the resonant frequencies of both simulated and measured return loss align and the return loss at the resonant frequency reaches -25dB, suggesting an excellent impedance matching (Fig. 6). A shift in the resonant frequency is observed when comparing simulated and measured return losses. This can be attributed to quenching of the conductive ink, resulting in a non-uniform (porous) deposition.

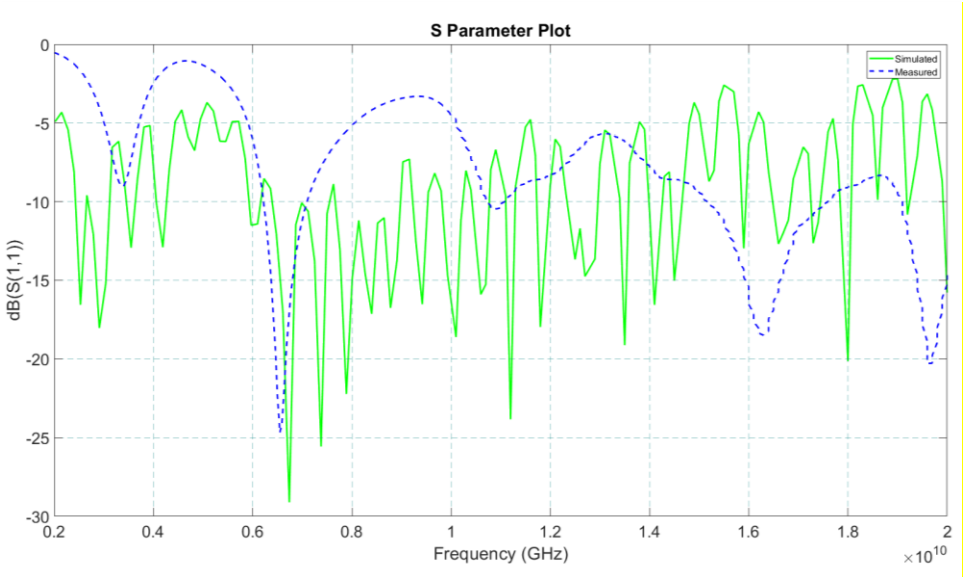

Figure 6. The simulated and measured return loss of the printed antenna-2.

Fig. 8(a, b) represents the current distribution of the printed antenna at 10 GHz and 20 GHz respectively. At 10 GHz, the current crowding is slightly observed thus resulting in an impedance mismatch. At the higher frequency end, i.e., at 20 GHz, two current minima are observed suggesting that the distance of separation negates the current crowding.

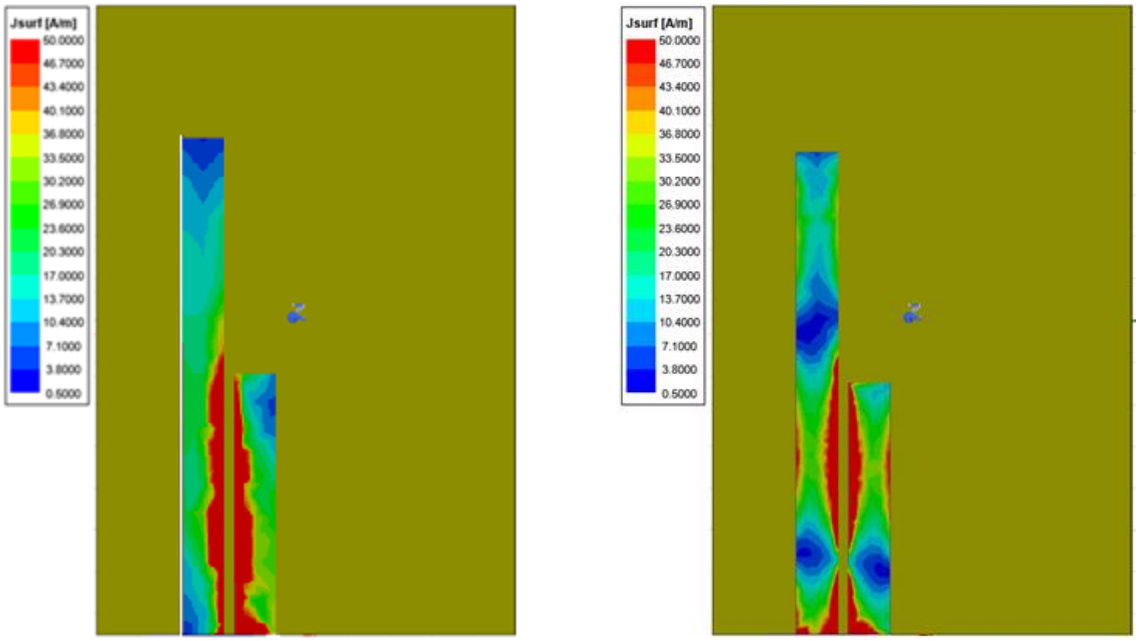

(a) (b)

Figure 8. Current distributions at (a) 10 GHz and (b) 20 GHz.

The radiation patterns of the proposed antenna have been simulated at specific frequencies. The H-plane radiation patterns and 3D polar plot of this printed antenna are simulated at 20 GHz in Figure 9(a). Similarly, the E-plane radiation patterns of this printed antenna are simulated at the same frequency as shown in Fig. 9(b). The nature of the radiation patterns is omnidirectional in H-plane and bidirectional in E-plane. It is also observed, as the frequency increases, the radiation patterns slightly vary which may be due to edge reflection, fractal geometry and high loss tangent of the substrate.

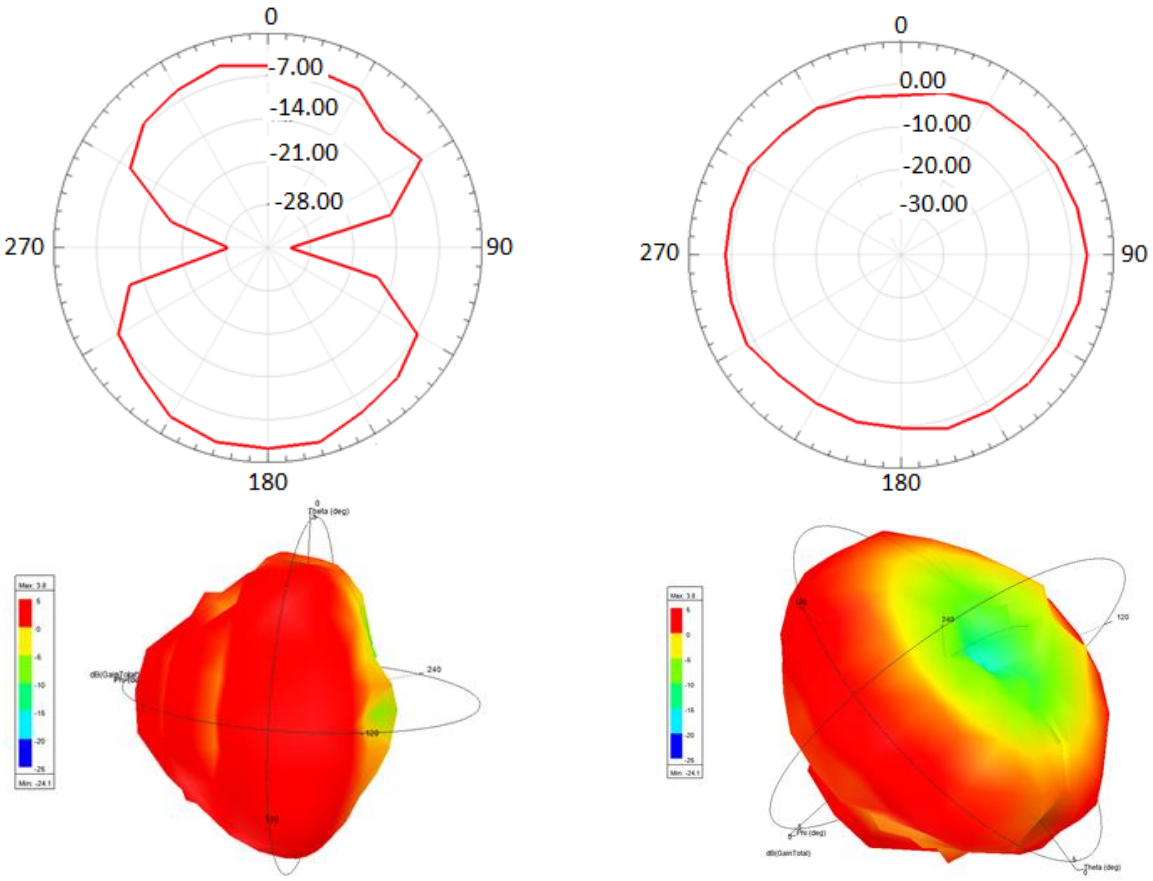

(a) (b)

Figure 9. Radiation patterns and the corresponding 3D polar plots in (a) E-plane and (b) H-Plane simulated at 20 GHz.

Conclusion

An Asymmetric-fed Coupled Stripline (ACS) antenna was printed on a FR4 substrate using the Voltera printing machine and obtained an impedance bandwidth ranging from 2 GHz to 20 GHz. The proposed microwave antenna was evaluated using Ansys HFSS and the results obtained were validated using the Keysight VNA. As well, the radiation patterns obtained were omnidirectional in H-plane and bidirectional in E-plane. The 20 GHz application frequency is attributed to Body-centric networks for patient monitoring in the 5G domain and orients well to the sustainable development goals (SDGs) transforming the world.

Acknowledgments

The authors would like to thank the U.S. Airforce ADMETE grant for providing financial supports. The authors would also like to thank Dr. Bhargavi Mummareddy, Mr. Khaled Alsharif and Ms. Krishna Ravali Jammalamadaka for supporting the antenna fabrication and technical help to carry out this work.

References

[1] L.-J. Xu, X. Jin, D. Hua, W.-J. Lu, and Z. Duan, "Realization of Circular Polarization and Gain Enhancement for Implantable Antenna", doi: 10.1109/ACCESS.2019.2963744.

[2] F. Ahmed, N. Hasan, and M. H. M. Chowdhury, "A compact low-profile ultra wideband antenna for biomedical applications," in *2017 International Conference on Electrical, Computer and Communication Engineering (ECCE)*, 2017, pp. 87–90.

[3] M. Särestöniemi, C. Pomalaza-Raez, K. Sayrafian, and J. Iinatti, "In-Body Propagation at ISM and UWB Frequencies for Abdominal Monitoring Applications," in *2021 IEEE International Conference on Communications Workshops (ICC Workshops)*, 2021, pp. 1–5.

[4] S. Markkandan, C. Malarvizhi, L. Raja, J. Kalloor, J. Karthi, and R. Atla, "Highly compact sized circular microstrip patch antenna with partial ground for biomedical applications," *Materials Today: Proceedings*, vol. 47, pp. 318–320, Jan. 2021, doi: 10.1016/J.MATPR.2021.04.480.

[5] D. Kahina, C. Mouloud, D. Mokrane, M. Faiza, and A. Rabia, "A Compact ACS-Fed Tri-band Microstrip Monopole Antenna for WLAN/WiMAX Applications," *Advanced Electromagnetics*, vol. 7, no. 5, pp. 87–93, 2018.

[6] R. Rengasamy, V. RajeshKumar, and K. v Phani Kumar, "An electrically small inverted L-shaped asymmetric coplanar strip-fed antenna with split-ring resonator for multiband applications," *International Journal of Communication Systems*, vol. 34, no. 17, p. e4983, 2021.

[7] S. L. Gunamony, G. J. Bala, S. M. G. Raj, and C. B. Pratap, "Asymmetric coplanar strip-fed electrically small reconfigurable 5G mid-band antenna," *International Journal of Communication Systems*, vol. 34, no. 15, p. e4935, 2021.

[8] R. Kumar and I. Srikanth, "Design of apollonian gasket ultrawideband antenna with modified ground plane," *Microwave and Optical Technology Letters*, vol. 54, no. 8, pp. 1793–1796, 2012.

[9] S. Itapu, "A 3–18 GHz UWB Antenna with modified feed-line," 2021.

[10] S. Itapu, "Semi-circular Slotted Monopole Antenna for Future Ultra-Wideband Applications," *CVR Journal of Science and Technology*, vol. 17, no. 1, pp. 44–48, 2019.

[11] T. K. Saha, T. N. Knaus, A. Khosla, and P. K. Sekhar, "A CPW-fed flexible UWB antenna for IoT applications," *Microsystem Technologies*, pp. 1–7, 2018.

[12] H. Shawkey and D. Elsheakh, "Multiband Dual-Meander Line Antenna for Body-Centric Networks' Biomedical Applications by Using UMC 180 nm," *Electronics*, vol. 9, no. 9, p. 1350, 2020.